Journal of Engineering
journal homepage: www.joe.uobaghdad.edu.iq
Number 9 Volume 26 September 2020

Mechanical and Energy Engineering

Experimental Study on Heat Transfer and Flow Characteristics in Subcooled Flow Boiling in a Microchannel

Suha A. Mohammed
Mechanical Engineering Dept.
University of Technology
Baghdad, Iraq
shawsuha@yahoo.com

Ekhlas M. Fayyadh
Mechanical Engineering Dept.
University of Technology
Baghdad, Iraq
20084@uotechnology.edu.iq

ABSTRACT

The current study presents an experimental investigation of heat transfer and flow characteristic for subcooled flow boiling of deionized water in the microchannel heat sink. The test section consisted of a single microchannel having 300µm wide nominal dimensions and 300µm height (hydraulic diameter of 300µm). The test section formed of oxygen-free copper with 72mm length and 12mm width. Experimental operation conditions spanned the heat flux (78-800) kW/m^2, mass flux (1700 and 2100) kg/m^2.s at 31˚C subcooled inlet temperature. The boiling heat transfer coefficient is measured and compared with existing correlations. Also, the experimental pressure drop is measured and compared with microscale pressure drop correlations. The results showed that higher mass flux leads to higher boiling heat transfer coefficient, and the dominant mechanism is convective boiling. Also, the experimental pressure drop decrease with increasing heat flux in a single-phase region while it increases in a two-phase region. Comparing the experimental results in the experimental condition range, showed that an existing correlation provides a satisfactory prediction of heat transfer coefficient and pressure drop.

Keywords: Microchannel subcooled boiling, heat transfer coefficient, pressure drop.

دراسة تجريبية على خصائص انتقال الحرارة والجريان في قناة مايكروية في ظروف الغليان تحت درجة التشبع

الخلاصة

تم في البحث الحالي اجراء دراسة تجريبية لانتقال الحرارة وخصائص الجريان للماء منزوع الايونات في حالة الغليان تحت درجة حرارة التشبع لقناة مايكروية. مقطع الاختبار يتكون من قناة مايكروية مفردة الاختبار بعمق (300 µm) وعرض (300 µm) وقطر هايدروليكي (300 µm). مقطع الاختبار مصـــــنوع من مـــــادة النحاس النقي وبالابعاد (72 mm)

*Corresponding author

Peer review under the responsibility of University of Baghdad.
https://doi.org/10.31026/j.eng.2020.09.12

Article received: 16/5/2019
Article accepted:7/9/2109
Article published:1/9/2020

طول و (12 mm) عرض. تمـــت التـــــجارب باستخدام فيض حراري بين kW/m^2 (78-800) ومعدل تدفق كتلي $kg/m^2.s$ (1700- 2100) ودرجه حراره دخول تحت الاشباع مقدارها (31˚C). تم قياس معامل انتقال الحرار في منطقة الغليان على طول القناة المايكروية ومقارنة النتائج مع العلاقات التجريبية الحالية. كذلك تم تسجيل النتائج العملية لهبوط الظغط على طول القناة المايكروية ومقارنتها مع العلاقات التجريبية الحالية. اظهرت النتائج ان معدل التدفق العالي يؤدي الى زيادة معامل انتقال الحرارة بالغليان مما يدل على هيمنة انتقال الحرارة بالحمل في منطقة الغليان كالية لانتقال الحرارة. كذلك هبوط الضغط يقل مع زيادة الفيض الحراري في المنطقة احادية الطور بينما يزداد في المنطقة ثنائية الطور. عند مقارنة النتائج ضمن نطاق ظروف العمل التجريبي، وجد أن العلاقات الحالية تعطي تنبؤًا مُرضيًا لمعامل انتقال الحرارة وانخفاض الضغط.

الكلمات الرئيسية: القناة المايكرورية، معامل انتقال الحرارة بالغليان، هبوط الضغط في القنوات المايكروية.

1. INTRODUCTION

In recent years, flow boiling through microchannels has attracted lot of interest because, in compact areas, it has a possibility for very elevated heat transfer rates. When wanting smaller rates of coolant flow by using the latent heat of the coolant, higher heat fluxes can be dispersed significantly by flow boiling as compared with its single-phase counterpart. The phase variation process happens at the fluid saturation temperature with higher temperature uniformity through the microchannel heat sinks, and that is another characteristic of the convective boiling process. In recent years, flow boiling heat transfer properties have been studied excessively in particular and fantastic efforts have been made to discover the heat transfer mechanisms in a small scale. However, various heat transfer properties were adduced under various experimental conditions such as working fluid, channel geometry, the used mass flux, and heat flux and saturation pressure, etc. Despite that, there are yet numerous existing problems that limit the additional implementation of the microchannel heat sinks, e.g., the large wall superheats at the onset of nucleate boiling (ONB), (**Lee and Mudawar, 2005**) the large wall-temperature difference between the channels and along with the channel as well as the instability of the two-phase flow. Subcooled boiling is predominately noticed in a micro-channel heat sink. This can maintain comparatively low wall temperature under highly subcooled conditions and prepare high heat transfer rates. When the surface is hot enough for the formation of bubbles, but the bulk liquid temperature is kept under its saturation value, subcooled flow boiling subsists. The onset of nucleate boiling, ONB is called the initial consistency of bubbles. Depending on to the classical theory, (**Tong and Tang, 1997)** as the bubbles that created at the wall proceed away from the developing saturation boundary layer, they will condense. Still, on the other hand, the heat transfer between the fluid and the wall will be impacted by the presence of these bubbles. During the high level of subcooling or low heat fluxes, just several nucleation sites are active, and a part of the heat is transferred by single-phase convection among patches of bubbles. This system is called partial nucleate boiling. Numerous nucleation sites are activated till fully developed nucleate boiling as the heat flux is increased when the surface turns into totally active for nucleation. Subsequently, the saturated nucleate boiling zone is entered when the saturation boundary layer develops and finally covers the whole channel as the bulk fluid is heated. Subcooled flow boiling is one of the most important parameters that affect the performance of the microchannel heat sink. **(Peng and Wang, 1993)** studied deionized water flow boiling in a rectangular evaporator of multi-microchannel made of stainless steel. The channel has an aspect ratio (W/H) equal to 0.86, 60mm length, and 0.65 mm hydraulic diameter. The experimental setup was an open-loop, and the liquid subcooling was changed from 40K to 70K. They described that although a fully developed nucleate boiling was noticed from the boiling curve, no bubbles were seen in the channel. They ascribed this phenom to the reality that the channel size was very less as compared with the "minimum evaporating space" wanted for the growth of the bubble. Also, they did not describe any influence for inlet subcooling and mass flux. **(Qu and Mudawar, 2003)** published convective boiling mechanisms by an inspected experimental study of 21 copper microchannels with 349 μm hydraulic diameter including (30-60) K inlet subcooling condition at range of heat fluxes (400-2400) kW/m^2 and (135-402) kg/m^2 mass fluxes using water as a working fluid. They found the dependency of heat transfer coefficient on mass flux and vapor quality but independent of heat flux. **(Galvis and Culham, 2012)** studied the water flow boiling characteristics in two various individual copper microchannels that have

the same length and aspect ratio but different hydraulic diameter (217 and 419) µm with two various inlet subcooling (50.7 K and 54.2 K). The tests were completed with a set of mass fluxes (340 and1373) kg/m^2, and (31.7 –1414) kW/m^2 heat fluxes. They mentioned that the nucleate boiling was the prevailing heat transfer mechanism because of the impact of heat flux upon the heat transfer coefficient, while the effect of mass fluxes on the heat transfer coefficient was insignificant.

(Mehmed, 2016) tested experimentally flow boiling heat transfer within a rectangular copper individual microchannel with 62 mm length, 1 mm width, and 0.39 mm height. The used working fluid was deionized water, the inlet subcooled and inlet pressure is 11℃ and 115 kPa, respectively, with a range of mass fluxes (200 -800) Kg/m^2.s and (56 - 865) kW/m^2 heat fluxes. A high-resolution, high-speed camera was also used to conduct a flow visualization. For whole mass flux values, the results show that unstable flow boiling happened to begin at the boiling onset. The local heat transfer coefficient totally relies on heat flux at extremely low mass and heat fluxes. During elevated mass flux, the impact of heat flux is not existed with little dependence on vapor quality after the entry region. The impact of mass flux was more complicated. **(Krishnamurthy and Peles, 2010)** investigated HFE-7000 subcooled flow boiling in a hydraulic diameter of 222 µm, with mass flux and heat fluxes range (350-827) kg/m^2, (100-1100) kW /m^2 respectively. Channels including an individual line of pin fins; significant heat transfer improvement was obtained and noted that through subcooled boiling, the local heat transfer coefficient was larger as compared with the similar single-phase flow. (**Callizo et al., 2007)** studied subcooled flow boiling heat transfer in vertical cylindrical tubes, including an internal diameter of 0.83, 1.22, and 1.70 mm for refrigerant R-134a experimentally. They examined the impacts of the inlet subcooling, channel diameter, mass flux, heat flux, and system pressure on the subcooled boiling heat transfer. They found that the wall superheats at ONB was discovered to be significantly higher as compared with that predicted with correlations for larger tubes. They found that a rise of the mass flux guides for early subcooled boiling and to arise in the heat transfer coefficient. The rise of the mass flux just happens in a slight improvement of the heat transfer for fully developed subcooled boiling. Smaller channel diameter, higher system pressure, and higher inlet subcooling are guide to preferable boiling heat transfer.

The above review indicates that there is no common conclusion about the dominant heat transfer mechanism(s) and the effect of heat and mass flux. Also, flow instability is a critical issue that should be highlighted in every boiling experiment. Thus, more research is still required in order to clarify and understand these fundamental points. The objective of the present work is to discuss the subcooled flow boiling heat transfer of deionized water heated in a single microchannel with 300µm hydraulic diameter and aspect ratio of 1. This test was done for various experimental conditions, mass fluxes (1700 and 2100) kg/m^2.s and heat fluxes range (78-800) kW/m^2 and 31˚C inlet subcooled temperature.

2. EXPERIMENTAL APPARATUS AND PROCEDURE

2.1 Experimental Setup

The experimental facility consists of a liquid tank, sub-cooler, peristaltic pump, turbine flow meter, pre-heater, test section, and inline filters. A schematic diagram and a plate of the experimental setup are displayed in **Figs. 1** and **2**, respectively. A chiller unit is used for cooling purposes in the sub-cooler and the condenser. Working fluid was deionized water. Vigorous boiling for about one hour was used for the degassing of the deionized water in the liquid tank. To release gases that are non-condensable to the atmosphere, the top valve of the condenser was opened. To separate all particles from the water a 7 µm filter was installed before the peristaltic pump in the suit. After that, the degassed water was introduced into the test section by pumping, and a pre-heater was used to control the working fluid inlet temperature. The microchannel test section is designed and machined from oxygen-free copper blocks; hence, the block of the microchannel test section has dimensions of 12 mm width, 25 mm height, and 72 mm length. Single microchannel having a length of 62 mm was cut into the top surface of the copper blocks between the 2 mm diameter inlet

and outlet plenums using milling machine at a feed rate of 10 mm/min. The typical dimensions of the microchannel are 300 µm width and 300 µm depth. These dimensions were measured utilizing an electro-microscope, and the actual values are (367 µm) for width and (269 µm) for height, as shown in **Fig.3.**

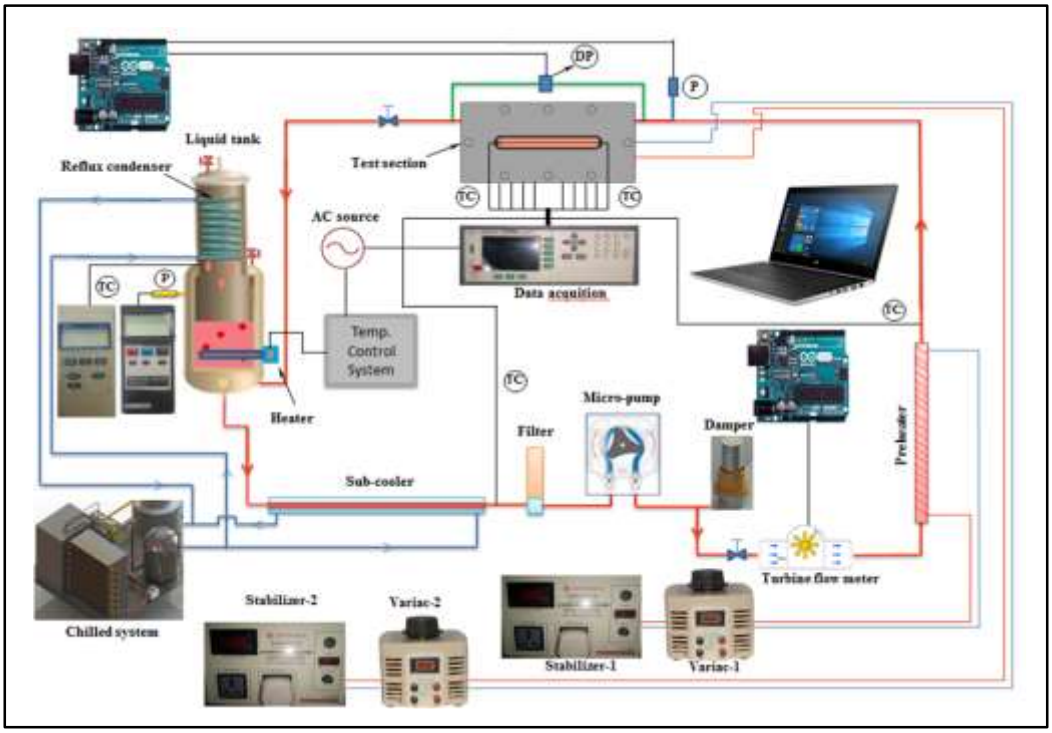

Figure 1. Schematic diagram of the experimental facility.

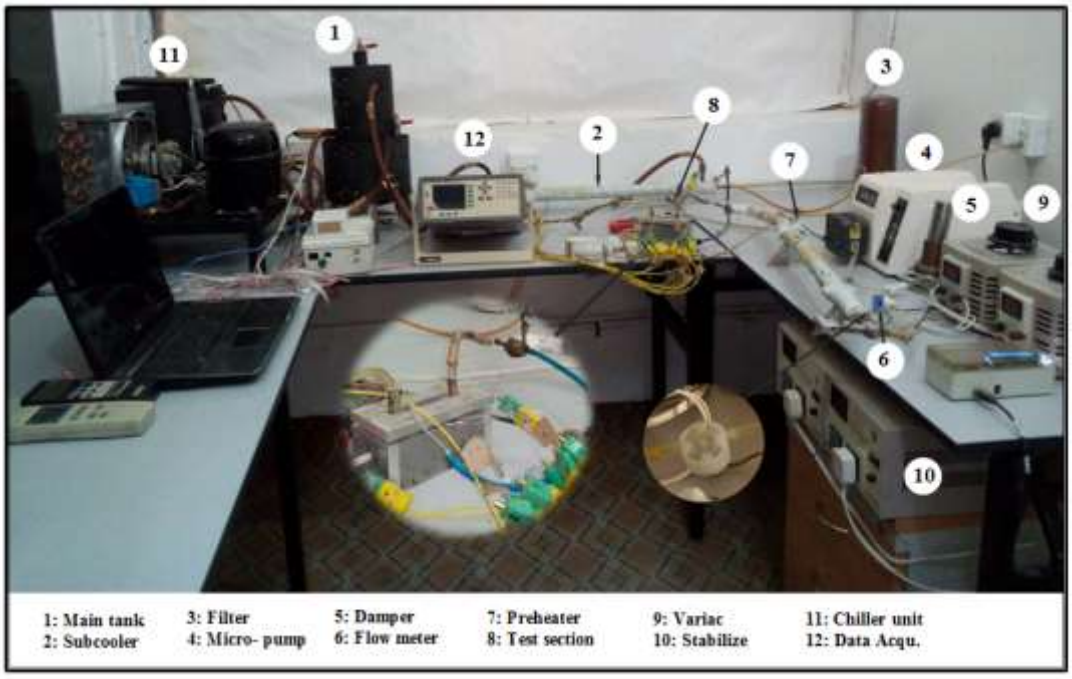

Figure 2. The plate of the experimental facility.

The surface roughness at the bottom of the Microchannel test sections was measured with AA3000 Scanning Probe Microscope (Atomic force Microscope AFM contact mode), which has multi–analysis: granularity and roughness.

The average surface roughness value is 0.011µm. **Fig.4** shows the roughness values that were evaluated over sample areas of 2cm x 1cm. A cartridge heater of 250 W heating power was inserted to the copper block at the bottom in a region parallel to the flow, which is placed in a drilled (8mm) hole within the copper block to supply the test section with the heating power. The local axial wall temperature was estimated in the 1 mm inner diameter and 6 mm depth hole at the portion of the block of copper. To determine the local heat transfer coefficient along the channel, six holes located over the axial side of the channel at an equidistance of 12.4 mm with 1 mm from the bottom of the channel to accommodate K-type thermocouples. Also, from the inlet of the channel with a distance of 24.8 mm, two holes were located vertically and 5 mm below the axial holes with an interval of 5 mm. To seal leak among microchannels and the top cover, on the top face of the microchannels, an O-ring slot was machined.

To reduce heat loss to ambient, the block is inserted into an insulation fiberglass sheet housing. Then the assembly is inserted into the housing component, which was designed and manufactured from stainless steel to accommodate the test section in the test loop. Between the stainless steel cover plate and the upper surface of the copper block, 4 mm thickness of transparent polycarbonate layer was sandwiched. Two holes were drilled at two locations in the top cover polycarbonate to accommodate thermocouple. One of them was at inlet plenum, while the other was at the outlet plenum of the microchannel test section to accommodate differential pressure drop across the microchannel test sections. **Fig. 5a** and **Fig.5b** present the main part of the test section and dimensions, respectively. During the present study, all thermocouples were calibrated with ± 0.5 K of uncertainty. A differential pressure transducer (26pcffT6D) was utilized for estimating the pressure drop, which was calibrated with an uncertainty of ±0.4 kPa. All information was listed after steady-state condition for 5 min using the Applent AT4532x data acquisition system.

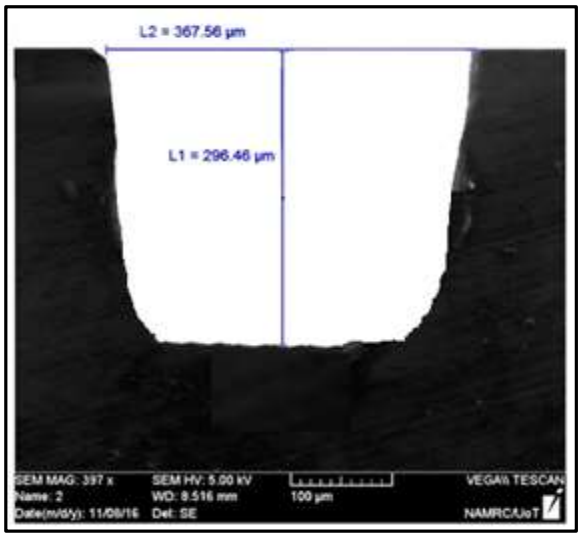

Figure 3. Microscope picture of microchannel

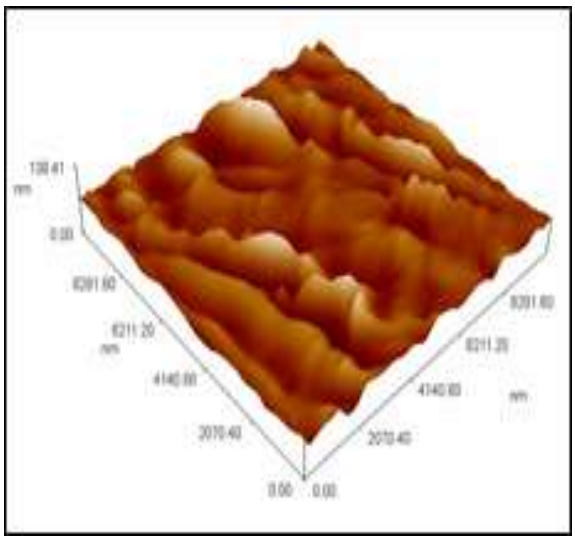

Figure 4. Surface roughness measurements of test-section.

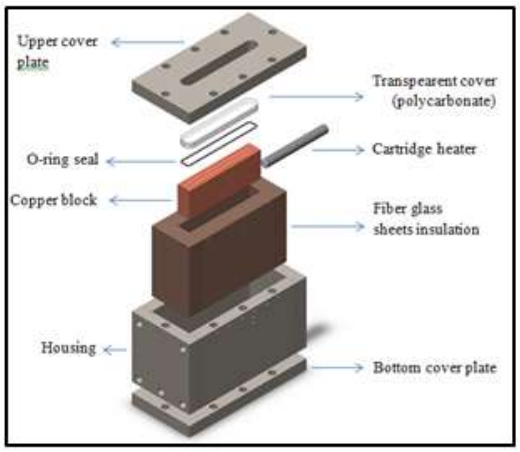

Figure 5a. Test-section constructions showing the main parts .

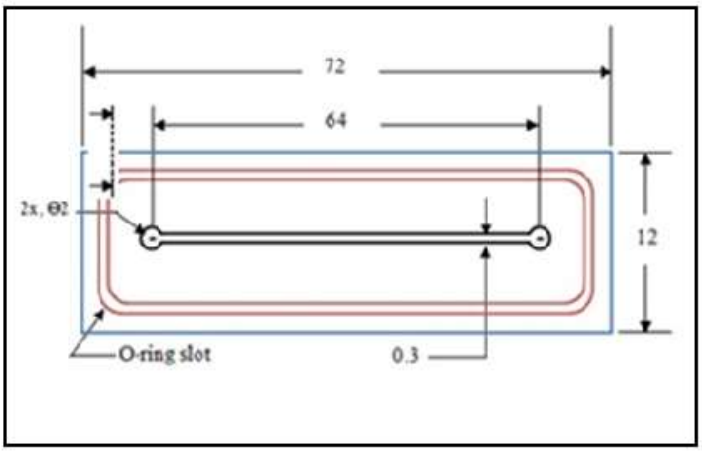

Figure 5b. Geometric design of microchanne (all dimensions in mm).

2.2 Experiments Procedures

Single-phase experiments were conducted in the current study for both adiabatic (friction factor calculation) and diabatic (heat transfer calculation) experiments. The deionized water temperature at the inlet of the test section in both experiments should be adjusted at (30)˚C at a Reynold's range of 700-2200 and (8) W input power for the diabatic experiment. Flow boiling experiments were conducted to obtain the flow boiling heat transfer coefficient, and flow boiling pressure drop data for the mass flux (1700, 2100) kg/m^2.s and heat flux (78-800) kW/m^2 at inlet subcooling 31 ˚C.

2.3 Data Reduction

2.2.1 Single-Phase flow data reduction

$\Delta P_{ch,}$ which is the net pressure drop over the microchannel for single-phase flow, is given by:

$$\Delta P_{ch} = \Delta P_{meas} - \Delta P_{loss} \quad (1)$$

ΔP_{meas} represents the total pressure drop among the inlet and exit plenums. The differential pressure sensor is used to measure it directly. ΔP_{loss} is the pressure loss due to the sudden enlargement and contraction and the inlet and outlet manifolds. It is described by **Eq.2**:

$$\Delta P_{loss} = 2\left(\frac{1}{2}\rho_l V_p K_{90}\right) + \frac{1}{2}\left(\rho_l V_{ch}(K_c + K_e)\right) \quad (2)$$

In **Eq. (2)**, Vp represents plenum liquid velocity, while Vch represents channel liquid velocity. The direction of entering and leaving flow in the channel is normal to the flow direction. Here, the loss coefficient according to 90° turns of the flow-through inlet and outlet plenums, is represented by K90, and that is specified by (**Philips, 1987)** as 1.2. For the channel entry and exit, sequentially, Kc is the sudden contraction loss coefficient, and Ke is the sudden enlargement loss coefficient. Tabular data introduced by **(Shah and London, 1978)** (can be used for their values by interpolating).

hsp(z) is the local single-phase heat transfer coefficient, and (Nu) represents the average Nusselt number. They are determined as:

$$h_{sp}(z) = \frac{q''}{T_w(z) - T_f(z)} \quad (3)$$

$$Nu = \frac{1}{L}\int_0^L \frac{h_{sp}(z)\, Dh\, dz}{k_l} \quad (4)$$

The 1D heat conduction equation used for the correction of the channel wall temperature Tw(z) at axial location z, is presented by **Eq. (5).** The liquid thermal conductivity is represented by k_l is, and Tf(z) is determined using **Eq. (6)** below considering uniform heat flux boundary conditions and depending on an energy balance. (q″) that is, the heat flux was described in **Eq. (7)**.

$$T_w(z) = T_{tc}(z) - \frac{q''\, t}{Kcu} \quad (5)$$

$$T_f(z) = T_i + \frac{q''\, wz}{\dot{m}\, C_p} \quad (6)$$

$$q'' = \frac{P - Q_{loss}}{A_{ht}} \quad (7)$$

where: the local thermocouple reading is represented by $T_{tc}(z)$, the thermal conductivity of copper represents by Kcu and the dimension from the channel bottom to the thermocouple position is represented by (t) and equal to 1 mm. The temperature of inlet fluid and the specific heat of liquid are represented by Ti and $C_{p,}$ respectively. The applied electrical power is symbolized by P, the heat transfer area represents by Aht, and it is described in **Eq. (8).** When there is no fluid inside the test section, an electrical power (P) applies to it to evaluate (Q_{loss}), which is the heat loss from the test section. Subsequent achieving steady state, the temperature difference among ambient and the bottom wall was listed for all heating power. After that, to achieve an equation to determine the heat loss (Q_{loss}) through single-phase and boiling tests, data obtained from the plotting of the applied power against this temperature difference.

$$A_{ht} = (2H + W)L \quad (8)$$

Where, H, W, and L are the high of the channel, the width and the length of it sequentially.

2.2.2 Two-Phase flow data reduction

The subcooled liquid state is the condition at which the fluid will coming in the channel. After that; the channel is separated into two regions, single-phase and two-phase. The region that begins from the channel entrance to the position of zero thermodynamic quality represents the single-phase region with length Lsub. Therefore, (L_{sat}) which represents the two-phase region length becomes

$$L_{sat} = L - L_{sub} \quad (9)$$

Next equations are used for the calculation of (L_{sub}), which is the length of the single-phase region, and it is determined iteratively.

$$L_{sub} = \frac{\dot{m}\, cp\, (T_{sat} - Ti)}{q''(2H+W)} \quad (10)$$

$$P_{sat}L_{sub} = P_i - \frac{2f_{app}\, G^2}{\rho_l D_h} L_{sub} \quad (11)$$

$$f_{app.} = \frac{3.44}{\mathrm{Re}\sqrt{L''_{sub}}} + \frac{f_{fd}\mathrm{Re} + \frac{k}{4\,L''_{sub}} - \frac{3.44}{\sqrt{L''_{sub}}}}{\mathrm{Re}\,(1+C(L''^{-2}_{sub}))} \quad (12)$$

T_{sat} is the liquid saturation temperature, while the apparent friction factor that was taken from **(Shah, 1978)** is represented by $f_{app.}$. **(Shah, 1978)** introduced the f.f_dRe, K(∞), and C as constant values that are mentioned in Eq. **(12)** for rectangular channels. (L''_{sub}) that is the dimensionless length in **Eq. (12)** can be calculated using **Eq. (13).** (f.fdRe) represents the fully-developed Poiseuille number. It is provided by **(Shah and London, 1978)** in **Eq. (14)** as a function of channel aspect ratio (β).

$$L''_{sub} = \frac{L_{sub}}{\mathrm{Re}\,D_h} \quad (13)$$

$$f.f_dRe = 24(1 - 1.3553\beta + 1.9467\beta^2 - 1.7012\beta^3 + 0.9564\beta^4 - 0.2537\beta^5 \quad (14)$$

β is the aspect ratio =1. In the two-phase section, the local pressure was supposed to reduce linearly with z (the axial length), and it can be determined from, **(Shah, 1978)**:

$$P_{sat}(z) = P_{sat}L_{sub} - \frac{z - L_{sub}}{L - L_{sub}}\Delta P_{tp} \quad (15)$$

The net pressure drop of the two-phase in the channel is measured from:

$$\Delta P_{tp} = \Delta P_{ch} - \Delta P_{sp} \quad (16)$$

(ΔP_{sp}) which is the pressure drop of the single-phase is able to be calculated depending on **Eq. (10)** and **Eq. (12)** that measured the single-phase region length (L_{sub}) and the apparent friction factor, respectively. Local heat transfer coefficient of the two-phase was determined as, **(Shah, 1978)**:

$$h_{tp}(z) = \frac{q''}{T_w(z) - T_{sat}(z)} \quad (17)$$

$T_{sat}(z)$ in **Eq. (17)** is, the local saturation temperature. It is determined depending on the local pressure presented by **Eq. (15).** x(z) is the vapor quality, and it was calculated by **Eq. (18)** and **Eq. (19)**.

$$i(z) = i1 + \frac{q''(2H+W)z}{m} \quad (18)$$

$$x(z) = \frac{i(z) - i_l}{i_{lg}(z)}(z) \quad (19)$$

Depending on the measured inlet temperature (Ti) and inlet pressure (Pi), the local inlet specific enthalpy i(z) is calculated. In **Eq. (19),** ilg(z) represents local liquid specific enthalpy, while ilg(z) represents local enthalpy of vaporization

3. RESULTS AND DISCUSSIONS

3.1 Single-Phase Results

The single-phase experiments were carried prior to boiling experiments to confirm the experimental system. The comparison between the calculated friction factor and the (**Shah and London, 1978)** correlation for developing and fully developed flow is represented in **Fig.6**. The figure proves that there is a good contract with correlations. **Fig.7** shows the experimental Nusselt number compared with the predictions from the correlations of **(Shah and London, 1978**; **Mirmanto, 2012; and Mehmed, 2016)**. It is obvious that the experimental values show a similar trend where Nusselt number increases with Reynolds number. However, the current experimental results agree very well with the experimental results of **(Shah and London, 1978)** for developing laminar flow.

3.2 Two-Phase Results

3.2.1 Boiling curve

The imposed wall heat flux is plotted against the wall superheat in boiling curves ($\Delta Tsat = Tw - Tsat$), which increases with increasing wall heat flux at constant mass flux. **Fig. 8** shows the classical boiling curve at the downstream location (z/l =0.6) for two different mass fluxes (1700 and 2100) Kg/m^{2}s. The figure is divided into two sections; the first one is the single-phase section where ($\Delta Tsat < 0$), and the second section is two-phase section where ($\Delta T_{sat} > 0$). The required heat flux for the commencement of boiling increases with increasing mass flux. Boiling occured early when the mass flux was lower.

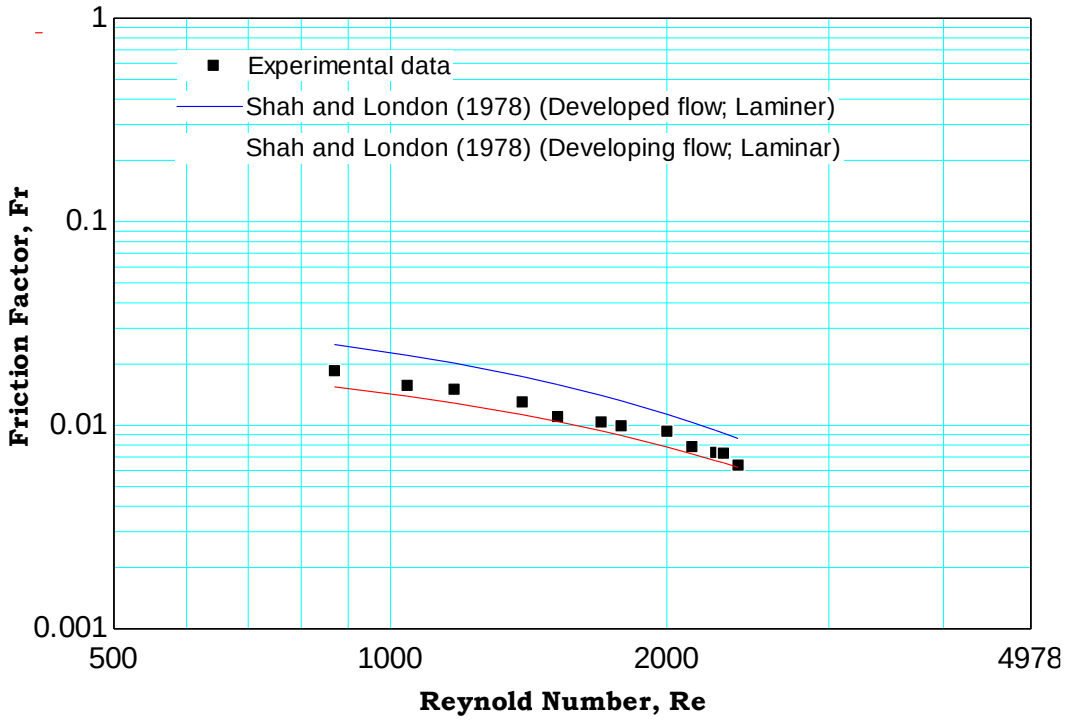

Figure 6. Single-phase results, Fanning friction factor versus Reynolds number.

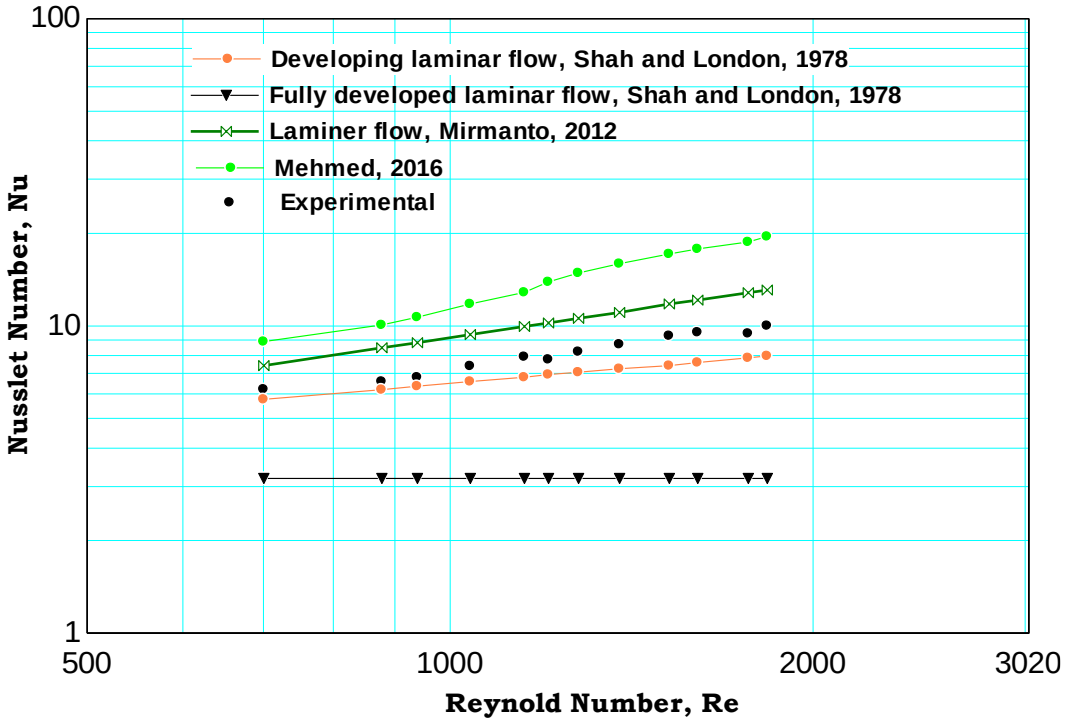

Figure 7. Single-phase results, Nusselt number versus Reynolds number.

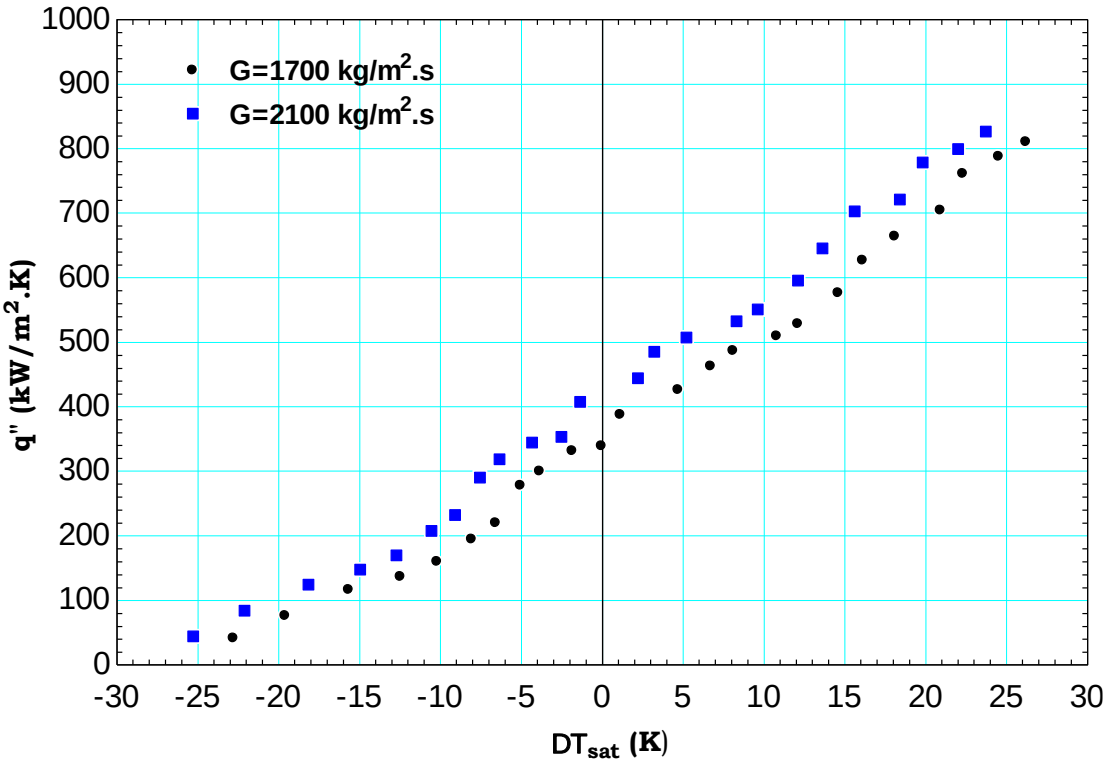

Figure 8. The impact of mass flux upon the boiling curve at 31˚C subcooled inlet temperature .

3.2.2 Effect of heat flux on heat transfer

In both micro and macro scale, the impact of heat flux represents an essential part in treating the case of representing predominant flow boiling heat transfer mechanism(s). The nucleate boiling mechanism is assumed to be predominant when the heat transfer coefficient does not vary with vapor quality and mass flux and increases with increasing heat flux. Also, convective boiling is considered to be the dominant heat transfer mechanism when the heat transfer coefficient does not depend on heat flux and increases with increasing mass flux and vapor quality. To determine the impact of the heat flux upon the local heat transfer coefficient, obviously for the test section, the heat fluxes are divided into two groups the first group with low heat flux values. In contrast, the others are considered as moderate to high heat fluxes. **Figs. 9** and **10** show the variation of the low heat flux and high heat flux on local two-phase heat transfer coefficient, respectively, at 1700 kg /m^{2}s mass flux and subcooled inlet fluid temperature is 31 ˚C. In **Fig.9,** the heat transfer coefficient remains in a single-phase region and it increases with increasing heat flux. The reason for that is the thermal boundary layer was not fully developed. Also, **Fig.9** shows that the heat transfer coefficient increased along the microchannel test part length for the fixed heat flux because of the effect wall temperature of microchannel increase in the axial direction due to the axial heat conduction effect.

Fig.10 depicted heat transfer coefficient of two-phase as a function of axial distance. Its shows that for the same point, increasing heat flux leads to decreasing the local heat transfer coefficient. The similar outcomes were obtained by a number of researchers such as, **(Burak Markal et al., 2016, Liu et al., 2011, as well as Lee and Mudawar, 2005)**, they reported that the reason for the decrease of two-phase heat transfer coefficient (htp) with increasing heat flux was due to partial dry out.

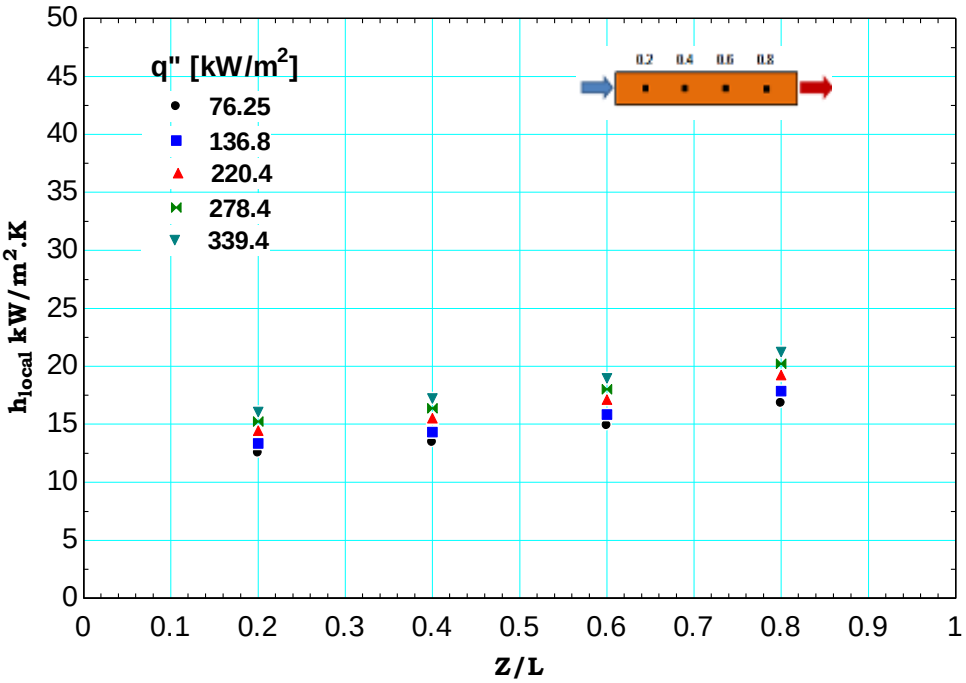

Figure 9. The impact of dimensionless distance from entry and low heat flux upon the Local heat transfer coefficient at a mass flux of 1700 kg/m^2.s and subcooled entry temperature of 31˚C .

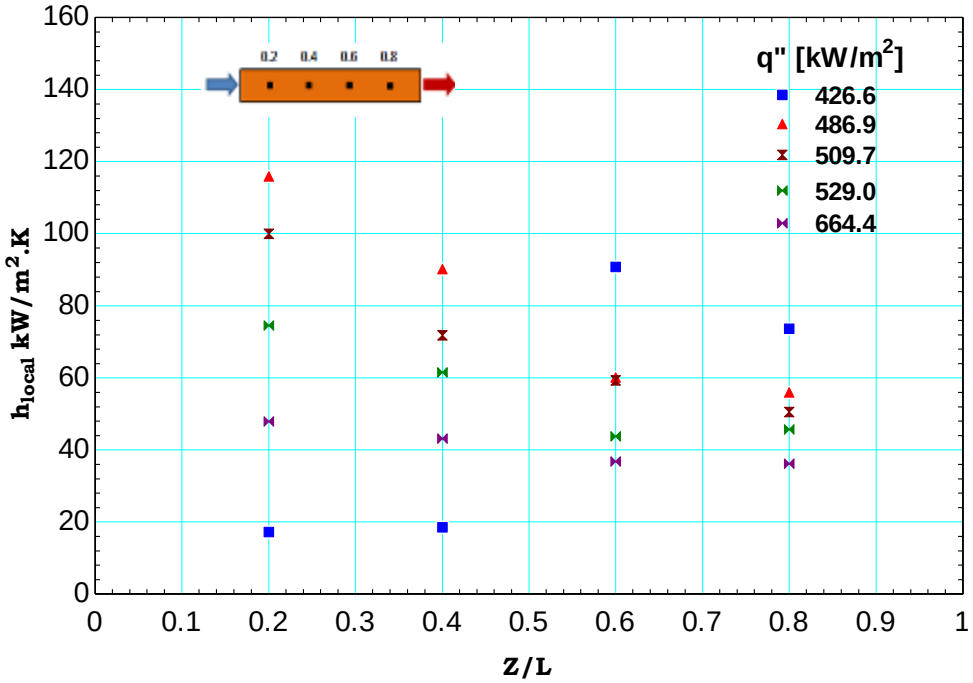

Figure 10. The impact of dimensionless distance from entry and high heat flux upon the Local heat transfer coefficient at a mass flux of 1700 kg/m^2.s and subcooled entry temperature of 31˚C.

3.2.3 Effect of mass flux on heat transfer

Fig.11 shows the variation of local heat transfer coefficient with heat flux for two mass fluxes at the position of (z/l = 0.6) for a thermocouple. The figure is divided into two regions subcooled flow boiling region and saturated flow boiling region. The two-phase region starts at the boiling incipience, where the peak value for the heat transfer coefficient is reached and then declines sharply. The figure also shows that the heat transfer coefficient increase by increasing mass flux for both the subcooled region and the saturated region at constant heat flux. And the boiling incipience delay for the higher mass flux and need higher heat flux for boiling incipience.

3.2.4 Heat flux and mass flux effect on subcooled flow boiling characteristics

The pressure drop across the microchannel heat sink considers an important parameter in microchannel design. **Fig. 12** represents the effect of heat flux on experimental pressure drop at (1700 and 2100) kg/m^{2}s mass flux at a subcooled degree of 31 ˚C. As seen in **Fig. 11,** at low heat fluxes range, the pressure drop is mainly due to all liquid single-phase flow, which is represented in decreasing pressure drop with increasing heat flux because of decreasing flow resistance due to the reduction of dynamic viscosity. While with increasing heat flux at the boiling incipience, the experimental pressure drop trend is different, where at constant mass flux the experimental pressure drop is increased with increasing heat flux due to increasing evaporation rate where the bubble expands toward the channel upstream, and that increased the resistance to incoming liquid flow. Also, the figure represents the effect of mass flux on experimental pressure drop, it seems that the experimental pressure drop increase with increasing mass flux. That is due to increasing the inertia force compare to the evaporation force with increasing mass flux, which leads to increasing the acceleration pressure drop component. Also, the frictional pressure drop component becomes higher at high mass flux increasing the number of bubble formation with

increasing mass flux in two-phase flow region lead to increasing pressure drop with increasing heat flux.

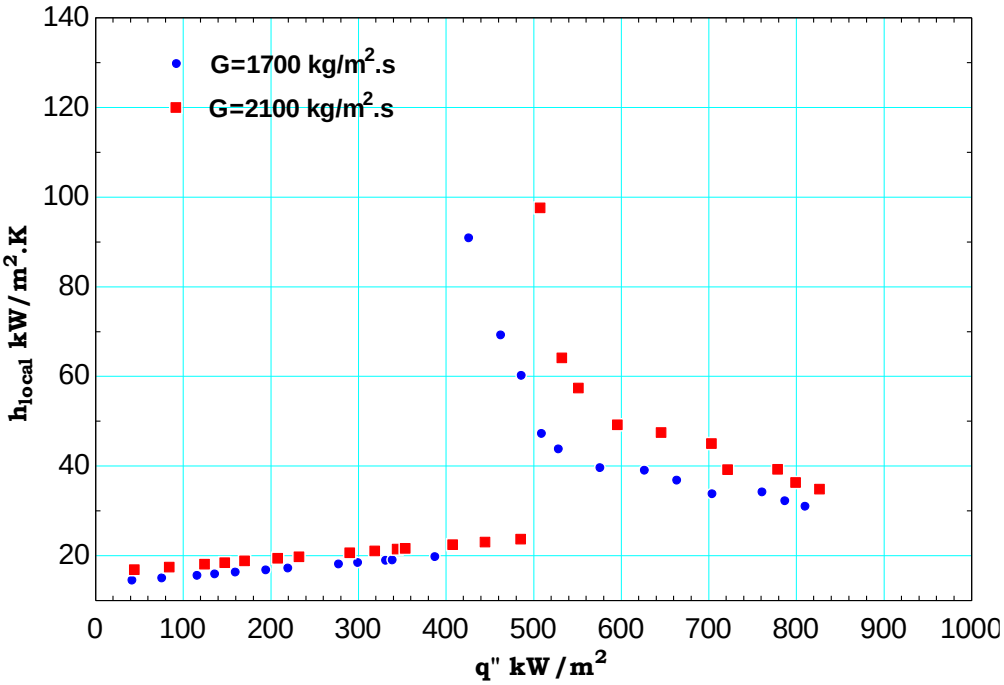

Figure 11. Mass flux effectiveness upon the local heat transfer coefficient at a subcooled inlet temperature of 31 ˚C.

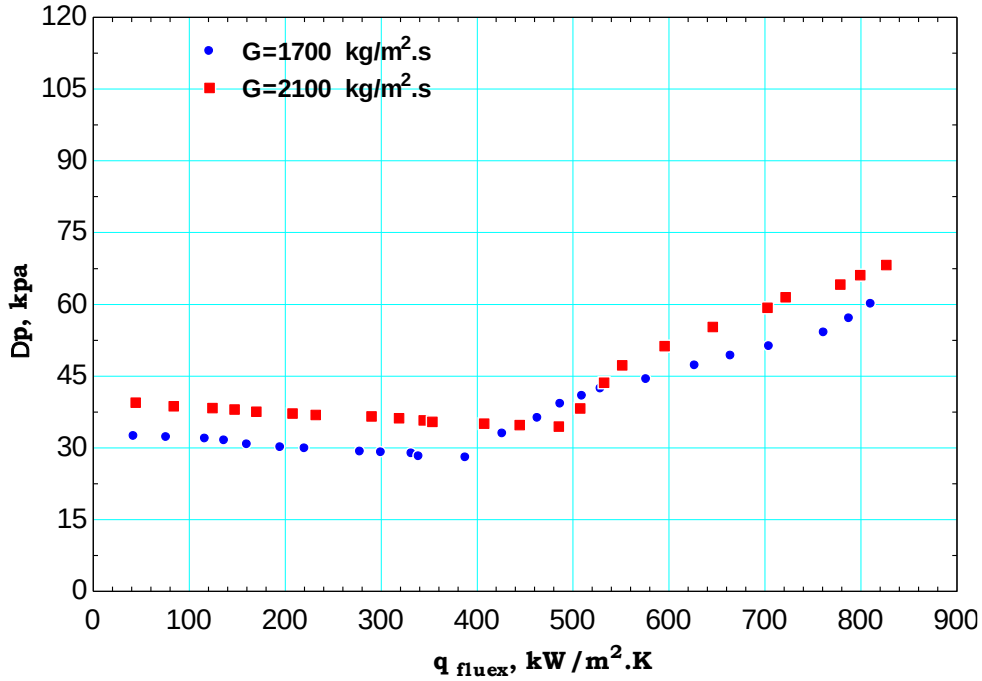

Figure12. Variation of experimental pressure drop with the variation of wall heat flux at 31˚C inlet degree of subcooled

3.3 Microscale heat transfer correlations

The heat transfer coefficient is difined by two correlations given by **(Lee and Mudawer, 2005)** and **(Mahmoud and Karayiannis, 2010),** is compared with the calculated heat transfer coefficient in the present work. The mean absolute error percentage (MAEP) is used for evaluating the accuracy of each correlation as follows

$$\text{MAEP} = \frac{1}{2}\sum \left|\frac{h_{exp} - h_{pred}}{h_{exp}}\right| * 100 \quad (22)$$

A relationship in a rectangular microchannel having a 0.35 mm hydraulic diameter for heat transfer of flow boiling is suggested by **(Lee and Mudawar, 2005)**. Data points for 318 heat transfer of water and refrigerant R134a are used to depend on it for the correlation. The correlations of (**Lee and Mudawar, 2005)** give the preferable correlations having minimal than 20% of mean absolute error, as shown in **Fig.13**. By utilizing the results of R134a, the correlation of **(Mahmoud and Karayiannis, 2010)** was advanced for microtubes. They adjusted the convective boiling enhancement factor and the nucleate boiling suppression factor. This correlation prediction was lower than that of **(Lee and Mudawar, 2005)**. This my be attributed to the state of the working fluid entering the microchannel which is subcooled in (**Lee and Mudawar, 2005),** which is similar to this study while it is saturated in **(Mahmoud and Karayiannis, 2010)** as shown in **Fig. 14**.

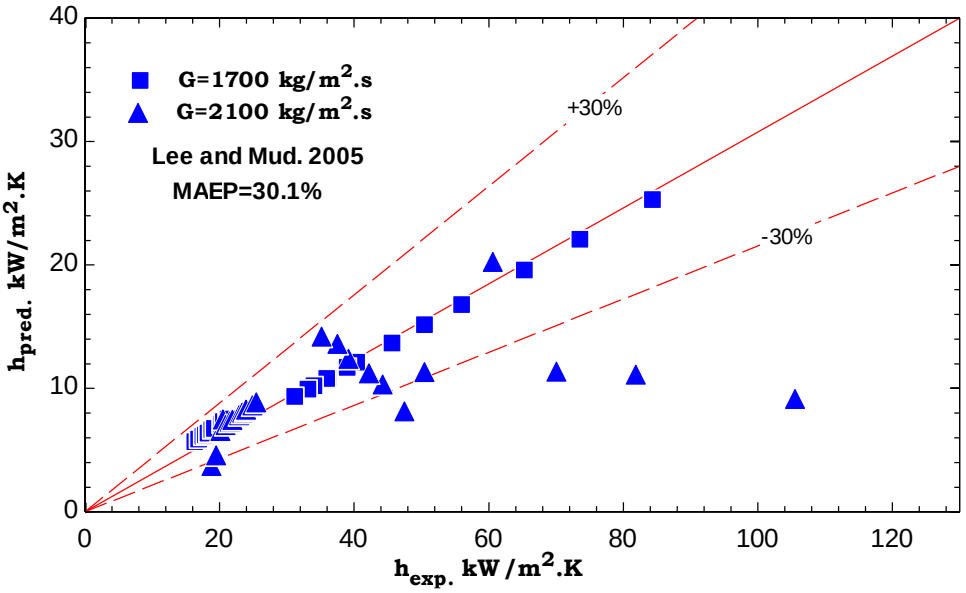

Figure 13. Comparison of experimental heat transfer data with **(Lee and Mudawer, 2005)** correlation at mass fluex 1700 and 2100 kg/m2.s and inlet subcooled 31 ℃ with MAEP 20%.

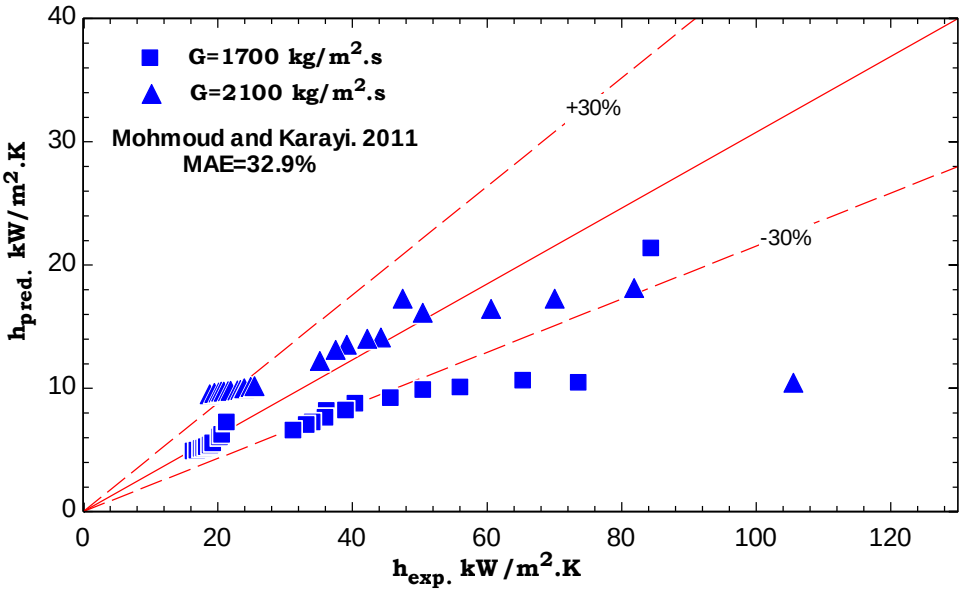

Figure 14. Comparison of experimental heat transfer data with **(Mahmoud, 2013)** correlation at mass flux 1700 and 2100 kg/m^2.s and inlet subcooled 31℃ with MAEP 30%.

3.4 Microscale pressure drop correlations

The experimental flow boiling pressure drop data for the microchannel heat sink were compared to micro-scale pressure drop correlation at the experimental condition; heat flux (78- 800) kW/m^2, mass flux (1700-2100) kg/m^{2}s, and 31˚C inlet degree of subcooling.
The mean absolute error percentage (MAEP) is used for evaluating the accuracy of each correlation as follows

$$\text{MAEP} = \frac{1}{2}\sum \left| \frac{\Delta P_{exp} - \Delta P_{pred}}{\Delta P_{exp}} \right| * 100 \quad (23)$$

Two correlation in microscale range were selected according to (**Warrier et al., 2002 and Qu and Mudawar, 2003; Warrier et al., 2002).** They proposed a correlation based on single-phase and both subcooled and saturated nucleate boiling experiments in parallel aluminum rectangular microchannel having 0.75 mm hydraulic diameter using FC-84 as working fluid and the heated length of 307.4 mm. The comparison with the experimental data depicted in **Fig. 15** shows that the correlation under predicts the data with MAEP values about 36.6%. The reasons may be due to using FC-84 as a test fluid that has lower surface tension and a smaller contact angle compared to the deionized water used in this study. Also, the poor prediction of **(Warrier et al., 2002)** may be due to fixing the Chisholm's constant at a value of 38, which may not be correct. The value of Chisholm's constant should vary according to the variation in the interaction between the phases. **(Qu and Mudawar, 2003)** developed a modification of the **(Mishima and Hibiki, 1996)** correlation of by incorporating mass velocity term and the effects of channel size. (**Mishima and Hibiki, 1996)** proposed a correlation based on experimental data with Dh (1.05-3.9) mm glass and aluminum vertical tubes and using air-water flow. Their data were well correlated by Chisholm′s correlation with a modified Chisholm′s parameter (C) as a function of inner diameter. In **(Qu and Mudawar, 2003)** study, the channels had 0.35 mm hydraulic diameter and using water as a

working fluid. **Fig. 16** depicts the global comparison with the experimental data. The correlation predicts the current experimental data with MAEP values about 24.4%. The good prediction of (**Qu and Mudawar, 2003)** correlation with the experimental data may be due to using deionized water as a test fluid which is the same of the current study also the subcooled inlet condition; beside the 0.35 mm hydraulic diameter which is close to the 0.3 the hydraulic diameter of this study.

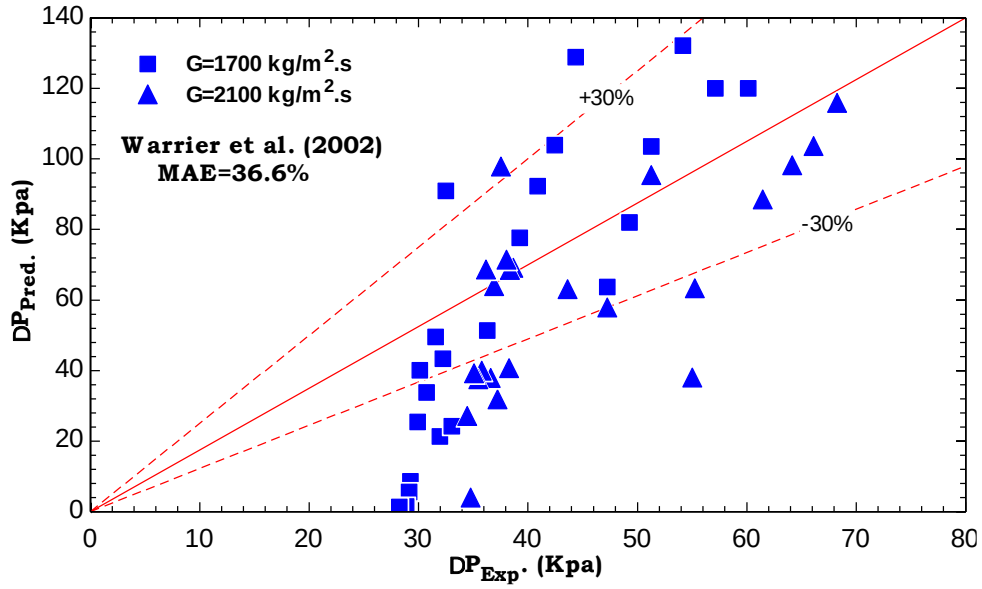

Figure 15. Comparison of experimental pressure drop results with **(Warrier et al., 2002)** correlation.

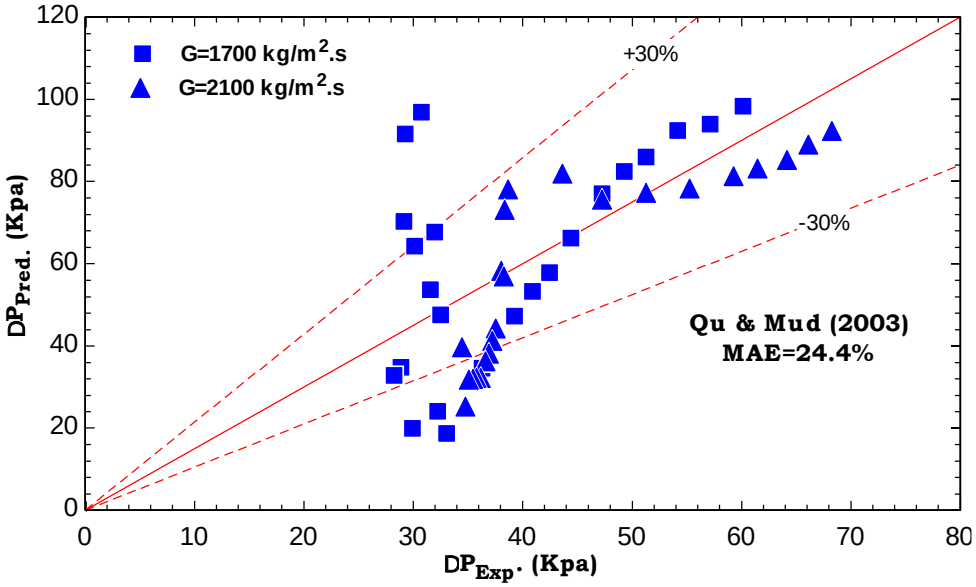

Figure 16. Comparison of experimental pressure drop results with **(Qu and Mudawar, 2003)** correlation.

4. CONCLUSIONS

The experiments of subcooled flow boing in a copper single microchannel heat sink utilizing deionized water were completed at 31°C inlet temperature, subcooled for two mass flux (1700 and 2100) kg/m^{2}s and heat flux range of (78– 800) kW/m^2. In this study, the main conclusions drawn from this study are: The correlations of fully developed flow and the conventional scale developing flow in the laminar regime were totally compatible with the experimental friction factor data. The impact of mass flux was clear on boiling curves, which shows that the mechanism is convective boiling. The results of heat transfer described that heat transfer coefficient based substantially on the heat flux where the two-phase heat transfer coefficient reaches peak value at boiling incipience. In contrast, in a single-phase region, the heat flux has a little effect on heat transfer. Also, the heat transfer coefficient is increased when the mass flux is increased.
The pressure drop in single-phase region decreased with increasing heat Flux, while it increased with increasing heat Flux in two-phase region.

5. REFERENCES

Callizo C. M., Björn P., Wahib O. 2007, *Subcooled flow boiling of R 134a in vertical channels of small diameter*, International Journal of Multiphase Flow, Issue 8(2007)822-832.

Chen, J.C.,1966, *A Correlation for Flow Boiling Heat Transfer to Saturated Fluids In Convective Flow*, Industrial and Engineering Chemistry, Process design and development, 5(3), 322-329,

Galvis, E. and Culham, R., 2012, *Measurements and flow pattern visualization of two phase flow boiling in single channel micro evaporator*, International Journal of Multiphase Flow, 42:52- 61.

Krishnamurthy, S., and Peles, Y., 2010, *Flow Boiling Heat Transfer on Micro Pin Fins Entrenched in a Microchannel*, ASME J. Heat Transfer, 132(4), 04-07.

Lee, J. and Mudawar, I., 2005, *Two-phase flow in high heat fluxes microchannel heat sink for refrigeration cooling applications: Part II-heat transfer characteristics*, International Journal of Heat and Mass Transfer, 48:941-955.

Liu, D., Lee, P.S. and Garimella, S.V., 2005, *prediction of the onset of nucleate boiling in microchannel flow*, International Journal Heat Mass Transfer, 48:5134- 5149, 2005.

Mahmoud, M. M., and Karayiannis, T. G., 2013, *Heat Transfer Correlation For Flow Boiling In Small to Micro Tubes*, Int. J. of Heat and Mass Transfer, 66, 553-574

Markal, B., Aydin, O. and Avci, M., *Effect of aspect ratio on saturated flow boiling in microchannels*, International Journal of Heat and Mass Transfer, 93:130 – 143, 2016.

Mehmed R. O., Mohamed M M., Tassos K., 2016, *Flow Boiling Heat Transfer In A Rectangular Copper Microchannel*, Journal of Thermal Engineering, Vol. 2, No. 2, pp. 761-773, July.

Mishima, K. and Hibiki, T., 1996, *Some characteristics of air-water two-phase flow in small diameter vertical tubes*, International Journal of Multiphase Flow, 22(4):703-712.

Mirmanto, M., *Single-phase flow and flow boiling of water in horizontal rectangular microchannels*, Ph.D. thesis, Brunel University London, London, UK, 2012.

Peng, X. F. and Wang, B. X., 1998, *Forced convection and boiling characteristics in microchannel*, Proceedings of 11th IHTC, 1:371-390.

Phillips, R.J., 1987, *Forced convection, Liquid Cooled, Microchannel Heat sinks*, MSc thesis, Massachusetts Institute of Technology, Cambridge, USA.

Qu, W. and Mudawar, I., 2003, *Measurement and prediction of pressure drop in two-phase micro-channel heat sinks,* International Journal of Heat and Mass Transfer, 46(15):2737-2753.

Qu, W. and Mudawar, I, 2003, *Flow boiling heat transfer in two-phase microchannel heat sinks-I, experimental investigation and assessment of correlation methods*, International Journal of Heat and Mass Transfer, 46:2755 – 2771.

Shah, R.K. and London, A. R., 1978, *Laminar flow forced convection in ducts,* Oxford Academic Press, New York, USA, Supplement 1 to Advances Heat Transfer.

Tong, L. S., and Tang, Y. S., (1997), *Boiling Heat Transfer and Two-Phase Flow, Second Edition, Taylor and Francis Ltd. London.*

Warrier, G. R., Dhir, V.K. and Momoda, L.A., 2002, *Heat transfer and pressure drop in narrow rectangular channels,* Experimental Thermal and Fluid Science, 26:53-64.